Loop-stabilized BAB triblock copolymer morphologies by PISA in water

Pauline Biais, Patricia Beaunier, François Stoffelbach, Jutta Rieger

Loop-stabilized BAB triblock copolymer morphologies by PISA in water

Pauline Biais[a], Patricia Beaunier[b], François Stoffelbach[a,*], Jutta Rieger[a,*]

[a] Sorbonne Université, CNRS, UMR 8232, Institut Parisien de Chimie Moléculaire (IPCM) Polymer Chemistry Team, 4 Place Jussieu, 75252 Paris Cedex 05, France

E-mail: jutta.rieger@upmc.fr; francois.stoffelbach@upmc.fr

[b] Sorbonne Université, CNRS, UMR 7197, Laboratoire de Réactivité de Surface (LRS) 4 Place Jussieu, 75252 Paris Cedex 05, France

FIGURE FOR TOC

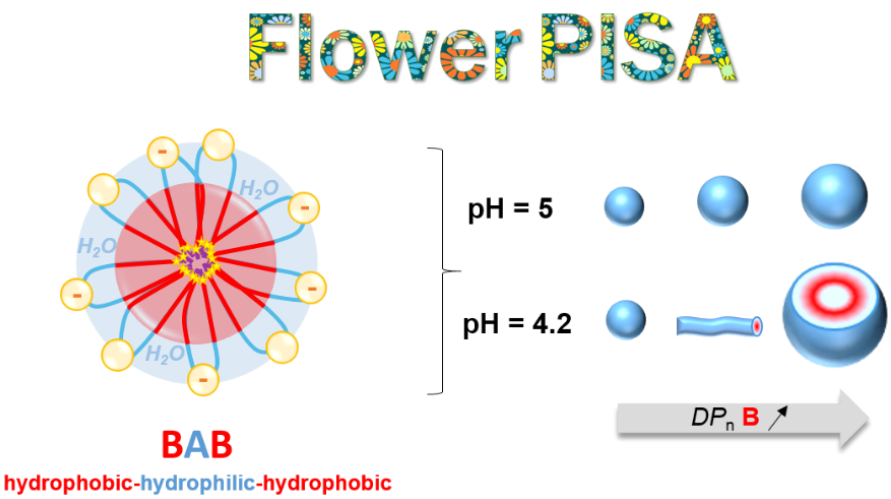

Text for TOC

Self-assemblies of BAB triblock copolymers are prepared by PISA *via* aqueous RAFT dispersion polymerization. The importance of charges in the middle of the hydrophilic stabilizer loops is highlighted.

Abstract

A straightforward strategy to synthesize in water, loop-stabilized particles *via* PISA is developed. These particular structures can in theory be obtained through the synthesis of amphiphilic BAB triblock copolymers, starting from a hydrophilic middle block A, which is chain extended in an aqueous PISA process by two hydrophobic external blocks B. For that purpose, symmetrical bifunctional poly(*N*,*N*-dimethylacrylamide) macroRAFT agents with a central benzoic acid group and an alkyl chain as Z group are used in the aqueous dispersion polymerization of diacetone acrylamide. For the first time, stable BAB flower-like particles are formed *via* PISA in pure water. It is shown that the colloidal stability and the resulting particle morphology (spheres, worms, vesicles) strongly depend on the degree of ionization of the central charge in the stabilizer loop, thus on the pH at which PISA is performed. Moreover, the influence of the length of the alkyl Z group (dodecyl and butyl alkyl chains) on the colloidal stability is studied.

1. Introduction

Over the past decade, polymerization-induced self-assembly (PISA) has become an efficient tool for the preparation of block-copolymer nanoparticles at high solids content, in both organic solvents and water.[1–7] In the PISA process amphiphilic block copolymers can be obtained through the use of reversible deactivation radical polymerization (RDRP) techniques, among which the reversible addition fragmentation chain transfer (RAFT)[8] has become the most popular and versatile one. In a first polymerization step, a "living" polymer, called macroRAFT agent, is synthesized in homogenous polymerization conditions. In the second step, the soluble macroRAFT is chain-extended with a solvophobic block in heterogeneous polymerization conditions, either through a dispersion or an emulsion polymerization mechanism. During the polymerization, an amphiphilic block copolymer is formed which self-

assembles into particles self-stabilized by the macroRAFT agent. Thus, no external stabilizer has to be added. Another big advantage of PISA is the possibility to form various morphologies, such as spheres, worms or vesicles, which paves the way towards new applications.[9–12] Higher order morphologies (*i.e.* worms, vesicles, lamellae) are not always observed and their formation markedly depends on various parameters, notably the polymerization process, the chemical nature and molar mass of the blocks, and the solvent used.[1,3,6,7] Another important parameter, that has received much less attention so far in PISA, should be the macromolecular architecture of the polymer chains. Hitherto there are only few reports in the literature comparing notably linear chains with stars or branched structures,[13,14] diblocks with triblocks or multiblocks[15–22] in PISA. Nonetheless, most of the studied systems are currently based on simple AB diblock copolymers, where A is the solvophilic, stabilizer block, and B is the solvophobic block. Another interesting class of linear block copolymers are BAB triblock copolymers, composed of a hydrophilic middle block A surrounded by two hydrophobic blocks B. In the past, such polymers have been synthesized in solution and showed to assemble in water into flower-like micelles or (reversible) physical gels through bridging of individual micelles.[23–26] If bridge/gel formation can be limited in PISA of BAB triblock copolymers, this process should be a straightforward method to produce loop stabilized particles. Actually, compared to linear chains polymer loops are known to exhibit very different stabilizing behavior. It was notably demonstrated that loops enhance the steric stabilization of surfaces and promote biopassivity and superlubricious behavior.[27]

To the best of our knowledge, very few studies report the synthesis of BAB triblock copolymer particles by PISA. Zhang group pioneered this field and studied the possibility to synthesize BAB triblock copolymer assemblies through a PISA process, carried out in mixtures of alcohols and water (80/20, w/w).[28–32] The first system they had studied compares the formation of poly(ethylene glycol)-*b*-polystyrene (PEG-*b*-PS) *AB* diblock and PS-*b*-PEG-*b*-PS *BAB* triblock copolymers in a methanol/water mixture *via* RAFT dispersion polymerization.[28,29]

For the BAB system a certain loss over control was observed, and large-sized aggregates of individual particles (so called gel-like networks) instead of small individual particles were formed due to bridge-formation between individual particles. In their following studies they replaced the stabilizing (PEG) macroRAFT agent with poly(*N*-isopropylacrylamide) (PNIPAM) and poly(4-vinylpyridine) (P4VP).[30–32] Using PNIPAM in a 80/20 ethanol/water mixture, well-defined PS-*b*-PNIPAM-*b*-PS triblock copolymers were formed in the course of the polymerization that self-assembled into spherical particles, stabilized by PNIPAM loops (such as in flower-like micelles), whose diameter increased during polymerization, *i.e.* with increasing length of the PS blocks.[30] More recently the group also explored BAB 4-arm star copolymers, (PNIPAM-*b*-PS)$_4$ in PISA.[31] Despite of the increased complexity of the macromolecular architecture, spherical particles were again formed, stabilized by PNIPAM loops. Whereas only spheres were obtained for these systems, the same group observed higher order morphologies (worms, vesicles and lacunary nanospheres) for PS-*b*-P4VP-*b*-PS copolymers synthesized in a methanol/water (80/20, w/w) mixture.[32] A strong impact of the number-average degree of polymerization (DP_n) of the P4VP stabilizer segment on the morphologies was notably highlighted. These examples show that flower-like amphiphilic BAB copolymer assemblies can be synthesized directly through PISA, but that the number of examples remains limited and that for BAB copolymers the parameters allowing the formation of higher order morphologies are far from being understood. Moreover, to the best of our knowledge, the synthesis of BAB triblock copolymers in water has never been reported yet.

In this context, this work aims at synthesizing BAB triblock copolymer assemblies directly in water *via* PISA giving rise to loop-stabilized particles. Poly(*N*,*N*-dimethylacrylamide) (PDMAc) and poly(diacetone acrylamide) (PDAAm) were selected as the hydrophilic (A) and hydrophobic (B) blocks, respectively. Indeed, PDMAc-*b*-PDAAm AB diblock copolymers have already been extensively studied in PISA, and it has been shown that a large variety of morphologies is accessible *via* aqueous dispersion polymerization.[33,34] Bifunctional

trithiocarbonate (TTC) RAFT agents with a benzoic acid derivative in their center and hydrophobic dodecyl chains or butyl chains as Z-end groups were selected for the synthesis of water-soluble TTC-PDMAc-TTC macroRAFT agents, which were then used in the dispersion RAFT polymerization of DAAm to yield PDAAm-*b*-PDMAc-*b*-PDAAm BAB triblock copolymer assemblies. In this paper three issues are addressed concerning (i) the possibility to prepare *in water*, loop-stablilized particles based on BAB copolymers, possibly of various morphologies, (ii) the role of the benzoic acid derivative at the symmetry point of the stabilizer PDMAc loops, and in particular its degree of ionization, on the morphology and colloidal stability, and finally (iii) the impact of the hydrophobic alkyl chain ends, in a BAB PISA system.

2. Experimental Part

Materials

N,*N*-dimethylacrylamide (DMAc, > 99%, Aldrich) was distillated under reduced pressure before use. 1,3,5-Trioxane (99%, Aldrich), 4,4'-azobis(4-cyanopentanoic acid) (ACPA, ≥ 98% Aldrich), 2,2′-azobis(2-methylpropionitrile) (AIBN, ≥ 98% Aldrich), sodium hydrogen carbonate ($NaHCO_3$, > 99.7% Aldrich), diacetone acrylamide (DAAm, 99%, Aldrich), *N*,*N*-dimethylformamide (DMF, VWR, Normapur) and 3,5-bis(2-dodecylthiocarbonothioylthio-1-oxopropoxy)benzoic acid ((C_{12}-TTC)$_2$-BA, 98% Aldrich) were used as received. 3,5-bis[2-(*n*-butyltrithiocarbonato)propionyloxy]benzoic acid ((C_4-TTC)$_2$-BA) was synthesized as reported before[35] with a purity of 97 %. Ethane-1,2-diyl bis(2-(((butylthio)carbonothioyl)thio)propanoate) ((C_4-TTC)$_2$-EG) was synthesized following a previously established protocol.[36] Deionized water was used for all the dispersion polymerizations.

Synthesis of the Poly(*N*,*N*-dimethylacrylamide) MacroRAFT Agents, (C_{12}-TTC-PDMAc)$_2$-BA and (C_4-TTC-PDMAc)$_2$-BA

Polymerizations of DMAc in DMF were initiated by AIBN at 70 °C, in the presence of the RAFT agents $(C_{12}\text{-TTC})_2$-BA and $(C_4\text{-TTC})_2$-BA (see **Scheme 1**). In a typical experiment (**Table S1**, entry **A**), the polymerization of 1.75 g of DMAc (1.77×10^{-2} mol) was carried out in 7 mL of DMF with 2.5 mg of AIBN (1.54×10^{-5} mol) and 127 mg of $(C_{12}\text{-TTC})_2$-BA (1.55×10^{-4} mol). A small amount (113 mg, 1.24×10^{-3} mol) of 1,3,5-trioxane was added as an internal reference for the determination of monomer consumption by ^{1}H NMR (by the relative integration of the protons of the 1,3,5-trioxane at 5.1 ppm and the vinylic protons of DMAc at 6.6, 6.3 and 5.7 ppm in $CDCl_3$). The solution was poured in a 10 mL septum-sealed flask and purged with argon for 40 min in an ice bath and heated up to 70 °C in a preheated oil bath under stirring. The kinetics of the polymerization was followed by ^{1}H NMR. After 133 min, the polymerization was stopped by immersion of the flask in iced water and exposure to air. After purification by twofold precipitation in diethyl ether and drying under reduced pressure, the yellow powder was characterized by ^{1}H NMR in acetone-d_6 and size exclusion chromatography (SEC) in DMF (+ LiBr, 1 g L^{-1}).

RAFT Dispersion Polymerization of Diacetone acrylamide in presence of Poly(*N*,*N*-dimethylacrylamide) MacroRAFT Agents

All the aqueous dispersion polymerizations of DAAm were performed at 70 °C at a stirring speed of 500 rpm, using a monomer content of 10 wt% with respect to the total latex and an initial initiator concentration of 0.76 mmol L^{-1}. The desired pH was adjusted using HCl and Na_2CO_3 diluted solutions. In a typical experiment (**Table 1**, entry **A-4**), 167 mg of DAAm (9.85×10^{-4} mol), 99 mg of macroRAFT agent $(C_{12}\text{-PDMAc})_2$-BA, **A** ($M_{n,LS}$ = 9.6 kg mol^{-1}, 1.0×10^{-5} mol) and 36 mg of 1,3,5-trioxane were dissolved in 0.60 g of a stock solution of ACPA in water (concentration of 0.5 g L^{-1} neutralized by 3 molar equivalent of $NaHCO_3$) and 0.82 g of deionized water. After being degassed 25 min with argon in an iced bath, the reaction mixture was heated up to 70 °C in an oil bath under stirring. The polymerization was stopped by

immersion in iced water and exposure to air. The conversions were determined by ^{1}H NMR in acetone-d_6 by the relative integration of the protons of the 1,3,5-trioxane at 5.1 ppm and the vinylic protons of DAAm at 6.3-6.1 and 5.5 ppm. The latex dispersion was characterized without further purification.

Characterization Techniques

pKa and ionization rate. The pKa value of a (C_{12}-TTC-PDMAc)$_2$-BA macroRAFT agent ($M_{n,RMN}$ = 5.0 kg mol^{-1}) was determined at 20 °C by acid titration with a NaOH solution at 0.01 M with a pH-M20 Lab pH-meter and a pH combined electrode using the Gran method[37]:

(Equation 1) $$[H_3O^+] * V\ (OH) = Ka * (Ve - V(OH))$$

with V(OH): added volume of NaOH
Ka: acid constant
Ve: full equivalence volume

(Equation 2) $$\alpha = \frac{Ka}{Ka + 10^{-pH}}$$

with α: ionization rate
Ka: acid constant

pH. The pH value of the aqueous dispersions was probed by a pH-meter (Mettler Toledo DL50 Graphix) using a micro-pH electrode (Mettler Toledo DGi101-SC).

NMR. DMAc and DAAm conversions were followed by ^{1}H NMR respectively in $CDCl_3$ and acetone-d_6 at room temperature with a Bruker 300 or 400 MHz spectrometer in 5-mm diameter tubes.

SEC. Size exclusion chromatography (SEC) analyses were carried out on two PSS GRAM 1000 Å columns (8 × 300 mm; separation limits: 1 to 1000 kg mol^{-1}) and one PSS GRAM 30 Å (8 × 300 mm; separation limits: 0.1 to 10 kg mol^{-1}) coupled with a differential refractive index (RI) detector, a UV detector and a light scattering (LS) detector. DMF (+ LiBr, 1g L^{-1}) at 60 °C was used as the mobile phase with a flow rate of 0.8 mL min^{-1}. Samples were filtrated on 0.2 µm pore-size membrane before injection. The dispersity ($Đ = M_w/M_n$), the number-average molar

mass (M_n), the weight-average molar mass (M_w) were calculated from the RI signals by a calibration curve based on PMMA standards with OmniSEC 5.11 software. The number-average molar mass ($M_{n,LS}$) of the macroRAFT agents was calculated from LS signal using a refractive index increment (d*n*/d*C*) of 0.081 mL g^{-1}.

DLS. Dynamic light scattering (DLS) measurements were performed at 25 °C to determine the *z*-average particle diameter (D_z) of 0.1 wt% diluted aqueous dispersions with a Zetasizer Nano S90 from Malvern (90 ° angle, 5mW He-Ne laser at 633 nm).

TEM. Transmission electron microscopy (TEM) was performed either on a JEOL JEM 2010 UHR microscope or on a JEOL JEM 2100Plus operating at 200 keV. The images were collected with a 4008 x 2672 pixel CCD camera (Gatan Orius SC1000). The aqueous dispersions were diluted in water to 0.1 wt% prior to analysis and then deposited at room temperature on a carbon-coated copper grid.

3. Results and Discussion

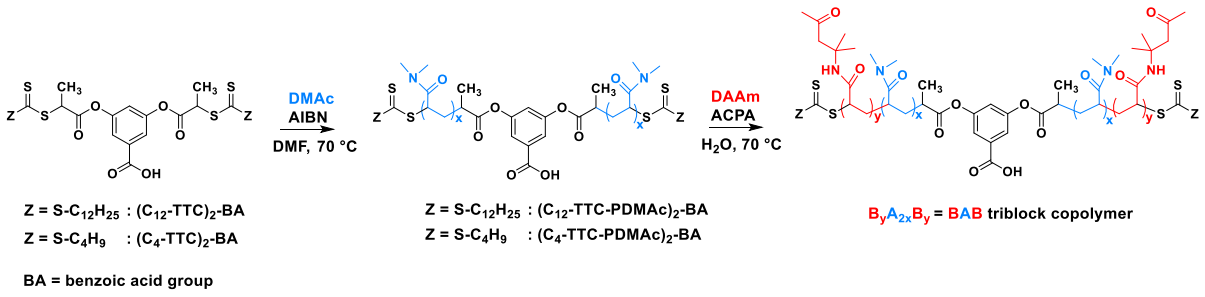

Scheme 1. Reaction scheme for the synthesis of the bifunctional PDMAc macroRAFT agents and their subsequent chain extension with DAAm to produce PDAAm$_y$-*b*-PDMAc$_{2x}$-*b*-PDAAm$_y$ BAB triblock copolymers *via* aqueous RAFT dispersion polymerization.

3.1. Synthesis of macroRAFT agents (C_{12}-TTC-PDMAc)$_2$-BA and (C_4-TTC-PDMAc)$_2$-BA

Two symmetrical bifunctional trithiocarbonate RAFT agents with the R group in the core and the Z group at the extremities (R = leaving group and Z = stabilizing group, Scheme 1) were used for the synthesis of PDMAc macroRAFT agents with a number-average molar mass (M_n) of about 10 kg mol^{-1}. The RAFT agents possess the same leaving group R, a 3,5-disubstitued benzoic acid (BA), but they differ in the length of the alkyl Z group. The first one, named (C_{12}-TTC)$_2$-BA and commercially available, has a C_{12} alkyl chain end-group and has already been used for the synthesis of triblock copolymer under homogeneous conditions.[38,39] The second one, (C_4-TTC)$_2$-BA, has a short C_4 alkyl chain and was synthesized according to a previously established protocol.[35] They were used in the solution polymerization of DMAc in DMF in presence of AIBN as an initiator.[16,40,41] The purified polymers were characterized by ^{1}H NMR and SEC (Table S1). In comparable polymerization conditions, the kinetics were similar for both RAFT agents and relatively high monomer conversions (~75%) were reached after 2.2 h (**Figure S1A** and **B**). Moreover, both RAFT polymerizations exhibited pseudo-first order kinetics with a very short induction period (< 20 min) (Figure S1B). Throughout the polymerization, the number-average molar masses (M_n) increased linearly with monomer conversion, and the molar mass dispersity ($Đ$) was generally below 1.3 (**Figure S1C**). These results are comparable to reported polymerizations of DMAc using bifunctional trithiocarbonate RAFT agent with the R group in the core.[25,42] Moreover, the experimental molar masses derived from SEC (using light scattering detection) and ^{1}H NMR were close to the theoretical ones indicating also a good control over the polymerization (Table S1). The two macroRAFT agents of comparable molar mass (~10 kg mol^{-1}) were used for the dispersion polymerization of DAAm in water.

3.2. Synthesis of PDAAm-*b*-PDMAc-*b*-PDAAm BAB copolymer assemblies in water

3.2.1. RAFT polymerization of DAAm using macroRAFT agent (C_{12}-TTC-PDMAc)$_2$-BA

Bifunctional *dodecyl* trithiocarbonate RAFT agent have already been used in the literature to synthesize BAB triblock copolymers by PISA in alcohol/water mixtures.[28–30,32] However the (C_{12}-TTC)$_2$-BA RAFT agent possessing a benzoic acid group in its center has never been used in PISA, at least to the best of our knowledge. In our first series of experiments, we tested the bifunctional dodecyl trithiocarbonate macroRAFT agent (C_{12}-TTC-PDMAc)$_2$-BA - derived from the (C_{12}-TTC)$_2$-BA RAFT agent - as a stabilizer and control agent in the aqueous dispersion polymerization of DAAm (Scheme 1). Polymerizations were carried out at 10 wt% (with respect to the total latex), and different degrees of polymerization (DP_n ~ 90, 180 and 260), *i.e.* different PDAAm molar masses, were targeted by varying the concentration of macroRAFT agent from ~2 to ~7 mmol L^{-1} (Table 1). In preliminary experiments, the aqueous solutions of the macroRAFT agent were slightly acidic (pH ~ 5, due to the benzoic acid unit), and for all further polymerizations pH was thus adjusted to 5.0 before polymerization to exclude any possible effects through different degrees of ionization of the benzoic acid group. All dispersion polymerizations reached high conversions (generally > 90% within ~ 140 min, Table 1) and stable homogeneous dispersions were formed (photographs in **Figure 1**, **A-1** to **A-3** at pH = 5). For the lowest PDAAm DP_n ($DP_{n,th}$ = 92), *i.e.* highest macroRAFT concentrations, a transparent free-standing gel was obtained (Entry **A-1**, Table 1, and photograph in Figure 1, **A-1**).

Table 1. Experimental Conditions and Results for the Dispersion Polymerizations of DAAm in the Presence of MacroRAFT Agents A, (C_{12}-TTC-PDMAc)$_2$-BA, and B, (C_4-TTC-PDMAc)$_2$-BA, in Water at Different pH at 70 °C[a]

Note: Dispersion polymerizations are named A-X and B-X to indicate the use of (C_{12}-TTC-PDMAc)$_2$-BA (A-X) and (C_4-TTC-PDMAc)$_2$-BA (B-X) respectively

Entry	pH	$[RAFT]_0$ (mmol L^{-1})	$[RAFT]_0/[ACPA]_0$	time (min)	conv.[b] (%)	$DP_{n,th}$[c] (PDAAm)	$M_{n,th}$[c] (kg mol^{-1})	$M_{n,PMMA}$[d] (kg mol^{-1})	$Đ$ [d]	D_z[e] (nm)	σ[e]	Morpho $_{TEM}$ [f]	$D_{n,TEM}$[f] (nm)
A-1	5.0	7.1	9.3	147	97	92	25.2	19.2	1.29	*m*	0.49	spheres	18
A-2	5.0	3.6	4.7	134	97	183	40.6	32.1	1.30	28	0.34	spheres	30
A-3	5.0	2.3	3.1	146	93	264	54.2	42.2	1.38	43	0.18	spheres	40
A-4	4.2	7.3	9.6	199	90	86	24.2	19.9	1.25	*m*	0.60	spheres	15
A-5	4.2	3.6	4.7	134	96	181	40.3	31.6	1.27	109	0.16	worms	23
A-6	4.2	2.3	3.1	170	95	269	55.2	43.1	1.27	297	0.28	vesicles	220
A-7	3.5	2.4	3.1	232	93	259	53.5	/ [g]	/ [g]	N.D.	N.D.	N.D.	N.D.
B-1	5.0	7.2	9.4	187	97	94	25.9	17.5	1.23	*m*	0.97	spheres	20
B-2	5.0	3.6	4.7	120	98	189	42.0	29.6	1.28	60	0.22	spheres	25
B-3	5.0	2.3	3.0	135	95	277	56.8	41,1	1.32	58	0.15	spheres	30
B-4	4.2	7.2	9.4	187	92	89	25.0	17.4	1.24	*m*	0.62	spheres	21
B-5	4.2	3.6	4.7	120	90	173	39.3	27.6	1.31	244	0.27	worms	22
B-6	4.2	2.7	3.6	154	89	219	47.0	N.D.	N.D.	N.D.	N.D.	N.D.	N.D.
B-7	4.2	2.3	3.0	150	93	271	55.8	/ [g]	/ [g]	N.D.	N.D.	N.D.	N.D.

[a] $[DAAm]_0$ = 10 wt%, $[ACPA]_0$ = 0.76 mmol L^{-1}. [b] Monomer conversion determined by ^{1}H NMR. [c] Theoretical number-average degree of polymerization, $DP_{n,th}$ (PDAAm), and number-average molar mass, $M_{n,th}$, calculated using the experimental conversion and using $M_{n,LS}$ for the PDMAc block (Table S1). [d] Number-average molar mass and dispersity, $Đ$, determined by SEC in DMF (+ LiBr 1g L^{-1}) with a PMMA calibration. [e] D_z is the Z-average sphere-equivalent diameter determined by dynamic light scattering, *m* stands for a multimodal size distribution and σ is the dispersity factor. [f] Morpho is the main morphology obtained and D_n is the number-average sphere, worm and vesicle diameter measured on TEM images. [g] multimodal molar-mass distribution. N.D. = not determined.

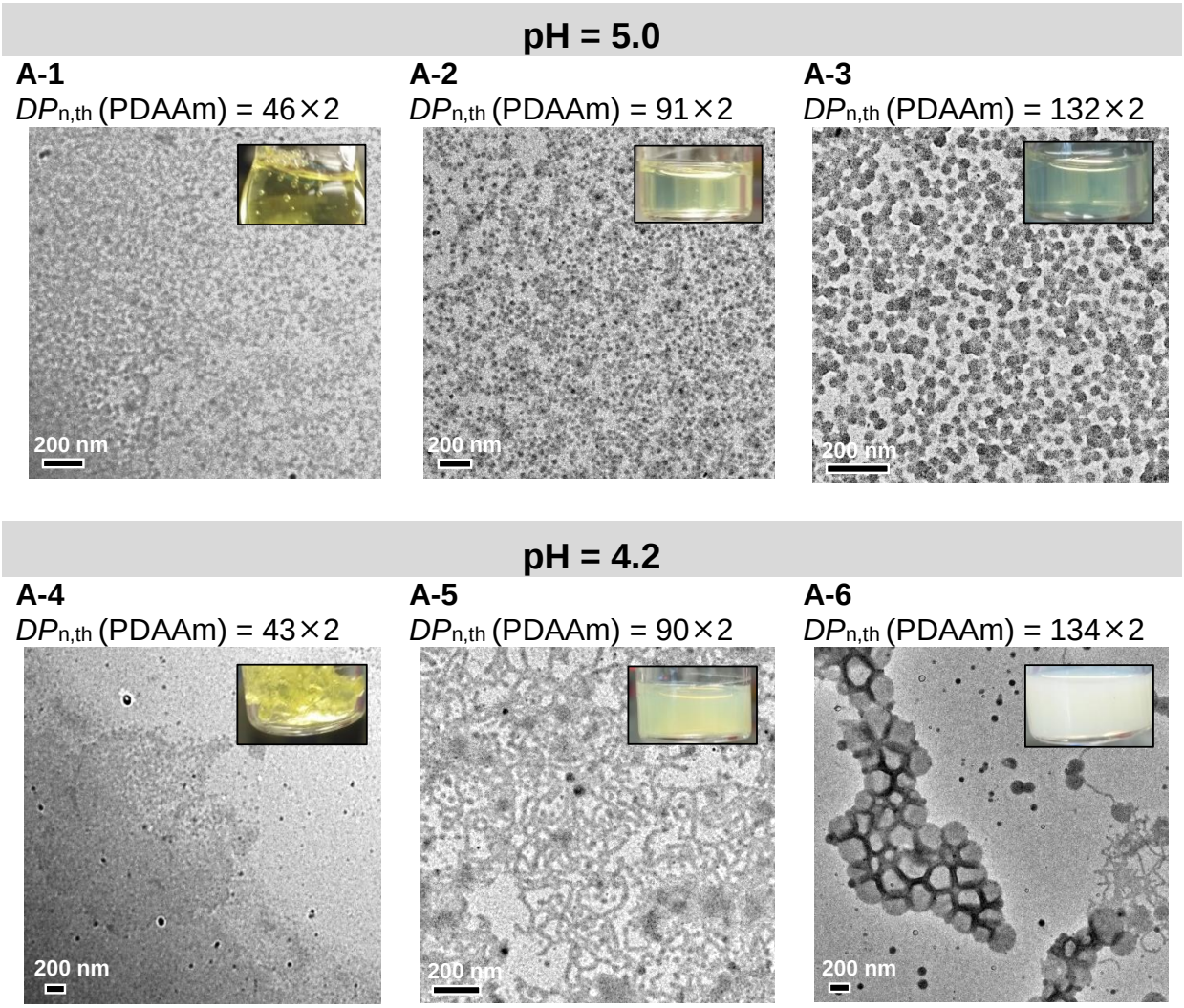

Figure 1. TEM images and photographs (inserts) for samples **A-1** to **A-6** prepared by the dispersion polymerization of DAAm with macroRAFT agent **A** $(C_{12}$-TTC-PDMAc$)_2$-BA at pH = 5.0 and pH = 4.2.

The control over the polymerization was investigated by SEC, and as reported in Table 1 and **Figure 2A**, independently of the targeted DP_n, a complete shift of the initial PDMAc macroRAFT agent signals towards higher molar masses was observed and relatively low dispersity values (< 1.4) were obtained, indicating the livingness of the polymerizations and the formation of block copolymers. SEC were generally symmetric and narrow, except for the experiment in which the highest concentration of macroRAFT agent **A** was used (shortest $DP_{n,th}$ (PDAAm) = 92, **A-1** in Figure 2A). This decrease in control compared to the other experiments

might be explained by the high viscosity of the dispersion, which should hamper the diffusion of the reactive species during the polymerization.

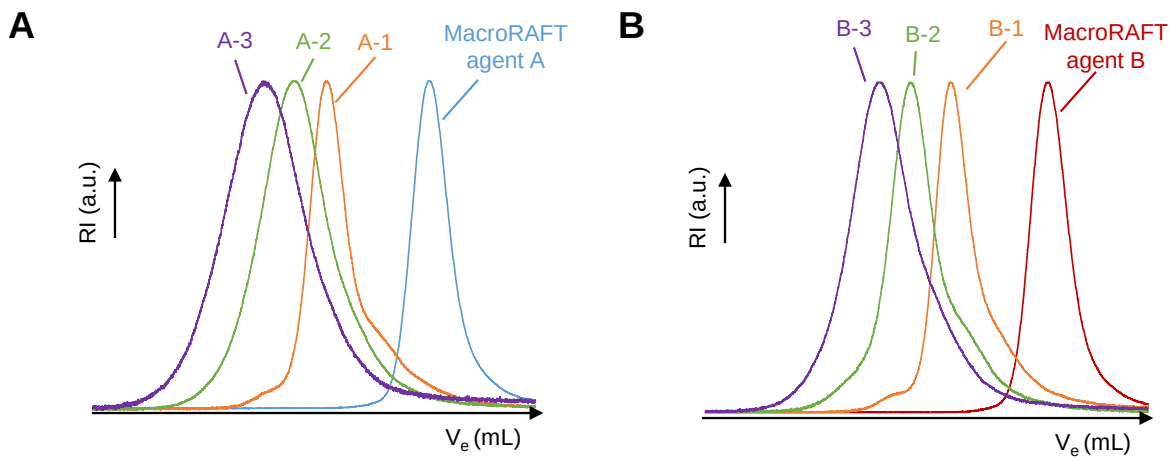

Figure 2. Normalized size exclusion chromatograms of macroRAFT agent **A**, (C_{12}-TTC-PDMAc)$_2$-BA and PDAAm-*b*-PDMAc-*b*-PDAAm copolymers **A-1**, **A-2**, **A-3** obtained by PISA at pH = 5.0 (A) and macroRAFT agent **B**, (C_4-TTC-PDMAc)$_2$-BA, and copolymers **B-1, B-2**, **B-3** obtained by PISA at pH = 5.0 (B).

TEM experiments of all the samples (**A-1**, **A-2** and **A-3)** revealed the formation of spherical particles, with diameters inferior to 50 nm (TEM images in Figure 1). As previously observed for diblock,[43] triblock[30] and star copolymers[16] an increase of the sphere diameter with the hydrophobic block length was observed by TEM and DLS measurements. However, no higher order morphologies, *e.g.* worms or vesicles, were observed, unlike for AB and (AB)$_n$ PDMAc/PDAAm block copolymers synthesized in comparable conditions.[16,33,40,44,45]

It is now established in PISA that higher order morphologies result from the fusion of individual particles formed in early stages of the polymerization.[1–3] It is also well known that this particle fusion can be inhibited by a too long stabilizer block, *i.e.* a too efficient steric stabilization.[16,44] Therefore, one possible explanation for the observed absence of the higher order morphologies in this series of experiments might be a too "efficient" stabilization by the long PDMAc

segments forming loops at the surface of the particles (Scheme S1). The total M_n of the used bifunctional PDMAc macroRAFT agent is ~ 10 kg mol^{-1}, *i.e.* in theory ~5 kg mol^{-1} at each side of the benzoic acid junction (assumed positioned in the middle of the stabilizing PDMAc loop). However, it has been previously shown for simple AB PDMAc/PDAAm diblock copolymers obtained by PISA in water, that higher order morphologies could be produced with PDMAc stabilizer blocks up to a M_n of 6 kg mol^{-1}.[40,44,46] The latter nanoparticles were stabilized by free linear chains, instead of loops as assumed for flower-like particles based on BAB copolymers. The absence of higher order morphologies might thus be related to the particular conformation of the stabilizer blocks (loops instead of linear chains) rather than to a too long molar mass. Interestingly, in the literature the stabilizing ability of polymer loops or cycles in particle stabilization[27,47,48] has already been compared with linear polymeric chains, revealing that the former particular polymeric architectures have a positive impact on the steric stability. An impact of the PDMAc conformation (linear *vs*. loop) on particle stabilization and particle fusion might thus be a plausible explanation for the observed differences between a BAB and AB system.

Finally, the presence of charges in the middle of the stabilizer loops, through the partial deprotonation at pH = 5 of the benzoic acid group in the middle of the PDMAc segment (see Scheme S1) may also play a crucial role in the particle formation mechanism. To understand further the system, we decided to explore in more details this latter parameter: Does a single central charge located at the middle of the stabilizer loops have an impact on particle stability and possibly on particle morphology?

3.2.2. Influence of the pH on the morphology obtained during the dispersion polymerization of DAAm in the presence of the (C_{12}-TTC-PDMAc)$_2$-BA macroRAFT

The impact of the degree of ionization of the benzoic acid moiety, present in the middle of the PDMAc block, was studied by varying the pH of the polymerization medium at which PISA

was performed. Firstly, the pK_a of the $(C_{12}$-TTC-PDMAc$)_2$-BA was measured by titration (**Figure S2**) and determined to be 4.6. The former polymerizations were all carried out at pH = 5.0, *i.e.* above the pKa corresponding to a degree of ionization of 72% (***Equation 2***). To study the influence of pH, a representative polymerization (**A-3**, $DP_{n,th}$ (PDAAm) ~ 260, Table 1) was repeated at different pH (4.2 and 3.5, **A-6** and **A-7**, Table 1), keeping all other polymerization parameters constant. Independently of the pH, all polymerizations reached high conversion (> 90%) (Table 1). As mentioned above, at pH = 5.0 (**A-3**, Table 1) a stable homogeneous translucent dispersion of tiny spherical particles had been obtained, exhibiting good polymerization control (**A-3**, Figure 2A). Decreasing the pH to pH = 3.5 resulted in a loss of particle stability and polymerization control (**A-7**, Table 1). At intermediate pH however (pH = 4.2), a stable, but milky dispersion was obtained, and no coagulum was observed (see photograph **A-6** in Figure 1). These results indicate that a certain degree of ionization of the benzoic moieties in the middle of the PDMAc loops is necessary to obtain a stable dispersion in our studied BAB system (Scheme S1). At pH = 5.0 and 4.2, the degree of ionization (72% and 28% respectively) is sufficient to stabilize the particles through electrostatic repulsion whereas at pH = 3.5 only 7% of the acid functionalities are deprotonated. At pH = 4.2, the molar mass dispersity remained low ($Đ$ < 1.3, experiment **A-6** in **Figure S3A** and Table 1), even though a shoulder at the lower molar mass side was observed. Contrary to the experiment at pH = 5.0, mainly vesicles ($D_{n,TEM}$ ~ 220 nm) instead of tiny spheres were obtained (**A-6**, Figure 1). When the total DP_n of the hydrophobic blocks was reduced to 181 and 86 (*i.e.* $M_{n,th}$ (total) ~ 40 and 24 kg mol^{-1}, **A-5** and **A-4**, Table 1), stable dispersions were again obtained at pH = 4.2 (see photographs **A-5** and **A-4**, Figure 1), and dispersities remained low ($Đ$ < 1.3), but the SEC chromatograms indicated again the presence of a secondary chain distribution of lower molar mass (see Figure S3A). As typically observed for PISA systems based on AB PDMAc/PDAAm diblock copolymers, the morphology changed with the decrease of the hydrophobic block length: worms and nanospheres were observed by TEM for the dispersion **A-5** and **A-4**

respectively (Figure 1). Comparison of these results with those of PDMAc-*b*-PDAAm diblock copolymers reported in the literature revealed that the different morphologies are obtained for similar DP_n ranges of the PDAAm blocks. For instance, Armes *et al.*[44] reported that with a PDMAc macroRAFT agent of DP_n = 43 (in our case $DP_{n,th}$ (PDMAc) = 86 with $DP_{n,th}$ = 43 at each side of the central benzoic acid group) and a $DP_{n,th}$ (PDAAm) > 130 vesicles were obtained, whereas mixtures of spheres and worms were obtained for $DP_{n,th}$ (PDAAm) < 92, which is comparable to the DP_n/block at which we observed vesicles and worms in the BAB system. Interestingly, the reverse triblock copolymer structures, that is ABA PDMAc-*b*-PDAAm-*b*-PDMAc copolymers, also formed the same morphologies for comparable PDMAc and PDAAm block lengths - even though these polymerizations were performed at higher solid contents.[16]

The crucial difference in morphology that we observed for polymerizations performed at pH = 5.0 and pH = 4.2 must be related to the reduction of negative charges present in the corona, thus the reduction of the electrostatic repulsion between particles promoting presumably particle fusion, which is a prerequisite for the formation of higher order morphologies.[3] In addition, with the increase of the protonation rate, the volume fraction of the hydrophilic PDMAc stabilizer block should be decreased and hence the packing parameter p,[49,50] might be increased. It should be noted that in the present work the influence of the pH on the morphology was studied by modifying the pH prior-polymerization. In the literature, the presence of a single charge at the chain end of non-ionic stabilizing polymers has already been reported to have a great impact on AB block copolymer morphologies obtained by PISA, but the morphological transitions were induced through pH variation post-polymerization.[51–53] Indeed, Armes *et al.* have shown that the degree of ionization of a single carboxylic acid group present at the α-end of a poly(glycerol monomethacrylate) stabilizer block can influence the morphologies of poly(glycerol monomethacrylate)-*b*-poly(2-hydroxypropyl methacrylate) (PGMA/PHPMA) AB block copolymer assemblies, previously obtained by PISA.[51,52] With increasing pH, for

$PGMA_{43}$-*b*-$PHPMA_{175-200}$ diblock copolymers a transition from vesicles to spheres and worms was observed,[51] while for $PGMA_{56}$-*b*-$PHPMA_{155}$ a transition from worms to sphere was observed.[52] The observed morphological transitions were explained by a conformational change of the stabilizing corona through protonation/deprotonation affecting the packing parameter p. However, for PDMAc-*b*-PDAAm AB copolymers, the same group has previously shown that the ionization of the carboxylic acid end-group was generally not sufficient to induce morphological transition.[44] Similarly, in our study, no significant changes could be observed when the pH of the dispersions was changed post-polymerization. Simply, a decrease to pH = 3.0 lead to the formation of some aggregates that were visible by the naked eye.

To conclude this part, a minimum degree of ionization of the benzoic acid middle group in the stabilizer is thus required to produce stable PDAAm-*b*-PDMAc-*b*-PDAAm BAB dispersions by PISA in water. The particles are flower-like particles, stabilized by PDMAc loops. It might be assumed that connections between individual particles exist as schematized in Scheme S1. Moreover, the type of morphology obtained depends not only on the length of the hydrophobic PDAAm block - as already observed before for PDMAc/PDAAm AB, ABA copolymers[16,33,40,44,45] - but also on the pH of the solution, *i.e.* the degree of ionization of a single benzoic acid group present in the PDMAc loops (see Scheme S1).

3.2.3. Influence of the alkyl chain length of the stabilizer group Z in the bifunctional macroRAFT agent on the aqueous dispersion polymerization of DAAm

All former experiments were carried out with the bifunctional telechelic dodecyl-terminated macroRAFT agent, $(C_{12}$-TTC-PDMAc$)_2$-BA. As mentioned above, hitherto only telechelic dodecyl-terminated macroRAFT agent have been used for the synthesis of BAB copolymers *via* PISA in alcohol/water mixtures.[28–32] Such telechelic water-soluble polymers possessing dodecyl chains are known to form individual or connected flower-like micelles, depending on the concentration and the polymer chain length.[42,54,55] It is thus reasonable to suspect that the

length of the alkyl chain (associative or not) could have an impact on PISA of BAB triblock copolymers, even though no significant differences in polymerization control and morphology had been formerly observed for AB diblock copolymers.[15]

We therefore synthesized the corresponding macroRAFT agent with a shorter and less hydrophobic alkyl chain - butyl instead of dodecyl - named $(C_4\text{-TTC-PDMAc})_2$-BA (macroRAFT agent **B**, Scheme 1 and Table S1). A series of dispersion polymerizations of DAAm was thus carried out in comparable conditions with this butyl-end-capped macroRAFT agent **B** (Table 1). Firstly, the $(C_4\text{-TTC-PDMAc})_2$-BA macroRAFT agent **B** was extended at pH = 5.0 to maintain the same degree of ionization as with the $(C_{12}\text{-TTC-PDMAc})_2$-BA macroRAFT agent **A**. Three different hydrophobic block lengths were again targeted ($DP_{n,th}$ ~ 90, 180, 270, entry **B-1**, **B-2** and **B-3** in Table 1) and stable dispersions were obtained (inserts in **Figure S4**). Similarly to the series with macroRAFT agent **A**, at this pH, a good blocking efficiency and low molar mass dispersities were determined by SEC (see **Figure 2B** and Table 1), and only *spherical* particles were formed (Figure S4). In conclusion at pH = 5.0, no significant effect of the alkyl chain length on the polymerization control, the morphology and particle stability was observed.

Next, the dispersion polymerization of DAAm with $(C_4\text{-TTC-PDMAc})_2$-BA was carried out at pH = 4.2 targeting similar DP_n (**B-4** to **B-7** in Table 1). The dispersions were stable and polymerizations reasonably controlled for **B-4** and **B-5**, but not for the experiments targeting the highest molar masses, *i.e.* typically the polymerizations using the lowest amount of stabilizer (samples **B-6** and **B-7**). Indeed, in the latter cases, instable, heterogeneous dispersions were obtained, and polymerization control was lost, as revealed by the bimodal SEC chromatogram in Figure S3B (Experiment **B-7**). For the shorter PDAAm blocks, however, stable dispersions were obtained, and essentially the same morphologies (spheres and worms) as with the linear triblock copolymers obtained in presence of the $(C_{12}\text{-TTC-PDMAc})_2$-BA macroRAFT agent, were formed (**B-4** and **B-5** in Figure S4). This difference in stability

observed at pH = 4.2 for the C_{12}- and C_4-end-capped macroRAFT agents is not fully understood yet and will be the topic of a forthcoming study.

Eventually, it might be noted that our hypothesis about the necessity to have a minimum amount of central charges to succeed PISA with PDAAm-*b*-PDMAc-*b*-PDAAm BAB copolymers, was further corroborated using a model PDMAc macroRAFT agent with an ethylene glycol unit, instead of a 3,5-disubstitued benzoic acid at its symmetry point, as stabilizer (see **Table S2**): independently of the tested polymerization conditions (DP_n, DAAm concentration), all dispersions presented a large amount of precipitate and bimodal SEC chromatograms (see **Figure S5**). The presence of charges in the stabilizer block is thus crucial for the successful synthesis of BAB block copolymer assemblies by PISA.

4. Conclusion

In this work, the possibility to prepare particles stabilized by loops instead of linear chains via PISA in water was studied. Our strategy relies on using symmetrical bifunctional trithiocarbonate macroRAFT agents with central R groups and Z groups at their extremities, leading therefore to a divergent polymerization mechanism and the formation of BAB triblock copolymers (with A the hydrophilic block, here PDMAc, and B the hydrophobic one, here PDAAm). We demonstrated for the first time that flower-like BAB particles, stabilized by PDMAc loops, can directly be produced *via* PISA in water, provided that a certain amount of charges is present in the middle of stabilizer PDMAc loops (here thanks to the presence of a central benzoic acid group in the RAFT agent). We further demonstrated that the degree of ionization of this single acid group plays a key role in the colloidal stability and also determines the particle morphology that is obtained. Whereas only spheres were obtained at pH = 5.0, at pH = 4.2, spheres, worms or vesicles could be formed - by increasing simply the length of the hydrophobic PDAAm blocks, just as for simple diblock PDMAc-*b*-PDAAm diblock copolymers. Finally, the impact of the hydrophobic alkyl chain length at the extremities of the

macroRAFT agents to produce BAB triblock copolymers was investigated in a comparative study using either C_{12} or C_4 end-capped macroRAFT agents. It was found that stable dispersions of spheres and worms could be obtained both for the C_{12} and C_4 end-capped macroRAFT agents. However, vesicles could only be formed with the C_{12}-end capped RAFT agent, at least in the studied conditions. We believe that the possibility to synthesize BAB copolymers in a straightforward manner by PISA – a system that has been overlooked so far in PISA - will pave the way to new applications of PISA, particularly the possibility to form gels and viscosity modifiers taking advantage of bridging between individual particles.

Acknowledgements: The authors thank Véronique Peyre (Sorbonne Université, PHENIX) for her advices to determine the pKa of the macroRAFT agent. Many thanks also to Olivier Colombani (Université du Maine, IMMM) for scientific discussion. J.R. thanks the Agence Nationale de la Recherche for funding (PISAForFilms project, ANR-17-CE09-0031-01).

Keywords: PISA, aqueous RAFT dispersion polymerization, BAB triblock copolymers, flower-like micelles, telechelic polymers

References

1 M. J. Derry, L. A. Fielding and S. P. Armes, *Prog. Polym. Sci.*, 2016, **52**, 1–18.
2 J.-T. Sun, C.-Y. Hong and C.-Y. Pan, *Polym. Chem.*, 2013, **4**, 873–881.
3 J. Rieger, *Macromol. Rapid Commun.*, 2015, **36**, 1458–1471.
4 Y. Pei, A. B. Lowe and P. J. Roth, *Macromol. Rapid Commun.*, 2017, **38**, 1600528.
5 B. Charleux, G. Delaittre, J. Rieger and F. D'Agosto, *Macromolecules*, 2012, **45**, 6753–6765.
6 S. L. Canning, G. N. Smith and S. P. Armes, *Macromolecules*, 2016, **49**, 1985–2001.
7 M. Lansalot, J. Rieger and F. D'Agosto, in *Macromolecular Self-assembly*, John Wiley & Sons, Inc., 2016, pp. 33–82.
8 J. Chiefari, Y. K. (Bill) Chong, F. Ercole, J. Krstina, J. Jeffery, T. P. T. Le, R. T. A. Mayadunne, G. F. Meijs, C. L. Moad, G. Moad, E. Rizzardo and S. H. Thang, *Macromolecules*, 1998, **31**, 5559–5562.
9 N. P. Truong, J. F. Quinn, M. R. Whittaker and T. P. Davis, *Polym. Chem.*, 2016, **7**, 4295–4312.

10 M. J. Derry, O. O. Mykhaylyk and S. P. Armes, *Angew. Chem. Int. Ed.*, 2017, **56**, 1746–1750.
11 R. Albigès, P. Klein, S. Roi, F. Stoffelbach, C. Creton, L. Bouteiller and J. Rieger, *Polym. Chem.*, 2017, **8**, 4992–4995.
12 K. L. Thompson, L. A. Fielding, O. O. Mykhaylyk, J. A. Lane, M. J. Derry and S. P. Armes, *Chem. Sci.*, 2015, **6**, 4207–4214.
13 X. Wang, C. A. Figg, X. Lv, Y. Yang, B. S. Sumerlin and Z. An, *ACS Macro Lett.*, 2017, **6**, 337–342.
14 J. Lesage de la Haye, X. Zhang, I. Chaduc, F. Brunel, M. Lansalot and F. D'Agosto, *Angew. Chem. Int. Ed.*, **55**, 3739–3743.
15 J. Rieger, W. Zhang, F. Stoffelbach and B. Charleux, *Macromolecules*, 2010, **43**, 6302–6310.
16 G. Mellot, P. Beaunier, J.-M. Guinier, L. Bouteiller, J. Rieger and F. Stoffelbach, *Macromol. Rapid Commun.*, DOI:10.1002/marc.201800315.
17 A. J. Convertine, B. S. Lokitz, Y. Vasileva, L. J. Myrick, C. W. Scales, A. B. Lowe and C. L. McCormick, *Macromolecules*, 2006, **39**, 1724–1730.
18 M. Chenal, L. Bouteiller and J. Rieger, *Polym. Chem.*, 2013, **4**, 752–762.
19 C. J. Mable, K. L. Thompson, M. J. Derry, O. O. Mykhaylyk, B. P. Binks and S. P. Armes, *Macromolecules*, 2016, **49**, 7897–7907.
20 A. H. Milani, L. A. Fielding, P. Greensmith, B. R. Saunders, D. J. Adlam, A. J. Freemont, J. A. Hoyland, N. W. Hodson, M. A. Elsawy, A. F. Miller, L. P. D. Ratcliffe, O. O. Mykhaylyk and S. P. Armes, *Chem. Mater.*, 2017, **29**, 3100–3110.
21 Y. Luo, X. Wang, Y. Zhu, B.-G. Li and S. Zhu, *Macromolecules*, 2010, **43**, 7472–7481.
22 C. J. Mable, L. A. Fielding, M. J. Derry, O. O. Mykhaylyk, P. Chambon and S. P. Armes, *Chem. Sci.*, 2018, **9**, 1454–1463.
23 A. J. de Graaf, K. W. M. Boere, J. Kemmink, R. G. Fokkink, C. F. van Nostrum, D. T. S. Rijkers, J. van der Gucht, H. Wienk, M. Baldus, E. Mastrobattista, T. Vermonden and W. E. Hennink, *Langmuir*, 2011, **27**, 9843–9848.
24 C. Charbonneau, M. M. De Souza Lima, C. Chassenieux, O. Colombani and T. Nicolai, *Phys. Chem. Chem. Phys.*, 2013, **15**, 3955.
25 K. Skrabania, W. Li and A. Laschewsky, *Macromol. Chem. Phys.*, 2008, **209**, 1389–1403.
26 C. Herfurth, A. Laschewsky, L. Noirez, B. von Lospichl and M. Gradzielski, *Polymer*, 2016, **107**, 422–433.
27 E. M. Benetti, M. Divandari, S. N. Ramakrishna, G. Morgese, W. Yan and L. Trachsel, *Chem. Eur. J.*, 2017, **23**, 12433–12442.
28 C. Gao, S. Li, Q. Li, P. Shi, S. A. Shah and W. Zhang, *Polym. Chem.*, 2014, **5**, 6957–6966.
29 C. Gao, J. Wu, H. Zhou, Y. Qu, B. Li and W. Zhang, *Macromolecules*, 2016, **49**, 4490–4500.
30 W. Wang, C. Gao, Y. Qu, Z. Song and W. Zhang, *Macromolecules*, 2016, **49**, 2772–2781.
31 Y. Qu, X. Chang, S. Chen and W. Zhang, *Polym. Chem.*, 2017, **8**, 3485–3496.
32 Y. Qu, S. Wang, H. Khan, C. Gao, H. Zhou and W. Zhang, *Polym. Chem.*, 2016, **7**, 1953–1962.
33 W. Zhou, Q. Qu, Y. Xu and Z. An, *ACS Macro Lett.*, 2015, **4**, 495–499.
34 Q. Qu, G. Liu, X. Lv, B. Zhang and Z. An, *ACS Macro Lett.*, 2016, **5**, 316–320.
35 N. Malic and R. A. Evans, *Aust. J. Chem.*, 2006, **59**, 763–771.
36 L. Voorhaar, B. De Meyer, F. Du Prez and R. Hoogenboom, *Macromol. Rapid Commun.*, 2016, **37**, 1682–1688.
37 G. Gran, *Analyst*, 1952, **77**, 661–671.
38 J. J. Gallagher, M. A. Hillmyer and T. M. Reineke, *ACS Sustain. Chem. Eng.*, 2016, **4**, 3379–3387.
39 M. Nasiri, D. J. Saxon and T. M. Reineke, *Macromolecules*, 2018, **51**, 2456–2465.

40 X. Wang, J. Zhou, X. Lv, B. Zhang and Z. An, *Macromolecules*, 2017, **50**, 7222–7232.
41 L. Sambe, K. Belal, F. Stoffelbach, J. Lyskawa, F. Delattre, M. Bria, F. X. Sauvage, M. Sliwa, V. Humblot, B. Charleux, G. Cooke and P. Woisel, *Polym. Chem.*, 2014, **5**, 1031–1036.
42 C. Herfurth, P. M. de Molina, C. Wieland, S. Rogers, M. Gradzielski and A. Laschewsky, *Polym. Chem.*, 2012, **3**, 1606–1617.
43 W. Zhang, F. D'Agosto, O. Boyron, J. Rieger and B. Charleux, *Macromolecules*, 2011, **44**, 7584–7593.
44 S. J. Byard, M. Williams, B. E. McKenzie, A. Blanazs and S. P. Armes, *Macromolecules*, 2017, **50**, 1482–1493.
45 C. A. Figg, R. N. Carmean, K. C. Bentz, S. Mukherjee, D. A. Savin and B. S. Sumerlin, *Macromolecules*, 2017, **50**, 935–943.
46 L. Zhang, Q. Lu, X. Lv, L. Shen, B. Zhang and Z. An, *Macromolecules*, 2017, **50**, 2165–2174.
47 D. Cao and J. Wu, *Langmuir*, 2006, **22**, 2712–2718.
48 G. Morgese, L. Trachsel, M. Romio, M. Divandari, S. N. Ramakrishna and E. M. Benetti, *Angew. Chem. Int. Ed.*, 2016, **55**, 15583–15588.
49 J. Israelachvili, *Intermolecular and Surface Forces*, Academic Press, 3rd edn., 2011.
50 A. Blanazs, S. P. Armes and A. J. Ryan, *Macromol. Rapid Commun.*, 2009, **30**, 267–277.
51 J. R. Lovett, N. J. Warren, S. P. Armes, M. J. Smallridge and R. B. Cracknell, *Macromolecules*, 2016, **49**, 1016–1025.
52 J. R. Lovett, N. J. Warren, L. P. D. Ratcliffe, M. K. Kocik and S. P. Armes, *Angew. Chem. Int. Ed.*, 2015, **54**, 1279–1283.
53 N. J. W. Penfold, J. R. Lovett, N. J. Warren, P. Verstraete, J. Smets and S. P. Armes, *Polym. Chem.*, 2016, **7**, 79–88.
54 M. A. Winnik and A. Yekta, *Curr. Opin. Colloid Interface Sci.*, 1997, **2**, 424–436.
55 E. Alami, M. Almgren, W. Brown and J. François, *Macromolecules*, 1996, **29**, 2229–2243.